
New Heater and Flux Gauge for the NBS Smoke Box

Richard L. Smith



United States Department of Commerce
Technology Administration
National Institute of Standards and Technology

Contents

I. Introduction	1
II. Heater	1
III. Gauge	6
IV. Radiation profile	6
A. Radiation profile technique	6
B. Experimental results	6
C. Estimation of average power	8
D. Effect of pilot burner's structure	14
V. Smoke chamber measurements	14
VI. Summary	15
References	16
Appendix 1: Manufacturer's Calibration Curve of FAA's Gauge	17
Appendix 2: BFRL "Calibration" of FAA's Gauge	18
Appendix 3: Manufacturer's Drawing of Tubular Heater	22
Appendix 4: Suggested New Wording for FAA's "Smoke Test for Cabin Materials"	24

Abstract

Improvements of the heater and the heat flux detector used in the FAA's Smoke Chamber test protocol are described. Heater designs were evaluated and two heaters were obtained and evaluated. This report covers various aspects of analysis and gives details on the heater that may provide a more uniform radiation field on the target specimen. The use of a smaller gauge, similar to the one used in the OSU calorimeter, in the smoke box for measuring the heat flux is discussed. Finally, a method that allows one to use the measurement of the radiation field at the center of the target specimen to infer the average radiation field over the specimen is presented.

I. Introduction

The objective of this project was to provide a faster and more accurate method of setting the heat flux in the NBS smoke density chamber for use by the FAA.

Reliable measurements of the rate of heat release and the generation of smoke are needed for the evaluation of aircraft cabin interior materials. FAA uses the ASTM E 662-83, "Standard Test Method for Specific Optical Density of Smoke Generated By Solid Materials." The FAA believes there is a significant variation in the incident heat flux over the surface of the specimen in practice compared to the standard's intended level. In addition FAA is not satisfied with the heat flux gauge prescribed in this test method, and they want one that can make a measurement faster and is easier to calibrate.

The constraints placed upon this project's objective by the FAA were that as much as possible NIST should not make changes to the test method that would bring into question the validity of the method using the new heater or detector or the usefulness of the previous data taken with NBS smoke chambers.

The expected results of this project are:

- 1) A demonstration of a prototype of a heater that will probably provide a more uniform radiation field on the target specimen;
- 2) A demonstration of the use of a gauge similar to the one used in the OSU (Ohio State University) calorimeter for use in the smoke box for measuring the heat flux; and
- 3) A method for using this heater and gauge that allows one to use the measurement of the radiation field at the center of the specimen to infer the average radiation field over the specimen.

The technical approach was that a series of designs for heaters were evaluated and two were selected and then their profiles were measured using a 6.35 mm (0.25 in.) aperture water-cooled Gardon gauge. A profile measurement technique was implemented for the new heaters and this Gardon gauge.

II. Heater

We have the following relevant quotation from the ASTM Standard E 662-83:

"From a scientific viewpoint, it would be desirable to have constant irradiance over all portions of the specimen. From a practical point of view, this was not feasible because size and heat input of the furnace would have to be greatly increased. It was considered, therefore, more practical to accept a modest nonuniformity of irradiance across the surface of the specimen. This is not defined in terms of radiance units, but rather by specifying the dimensions of the furnace geometry and the specimen spacing. Thus radiant configuration geometry was selected as a means of specifying the variability of surface irradiance. The average irradiance specified in the test method is that measured by

the radiometer describe in the standard, an instrument sensitive only to the 1 1/2 in. diameter central area of the specimen holder." [1]

Thus the persons drafting this standard recognized that a constant uniform field over the sample was not practical. Therefore, they tried for a reasonable compromise. What is desirable for this standard is that all parties using this test method have the same shaped radiation field on the target and the same power density at corresponding points. Currently heaters with different configuration for the radiating surfaces are being used. For example, often when the heating coil sags or is otherwise loose, a glob of heat resistant cement is applied over the heater to hold it in place. This produces unpredictable differences in the radiation pattern on the target.

In order to investigate the effect of various heater designs upon the radiation pattern a computer program was written that would compute the radiation pattern on the target. In the following summary of the results of our calculations for various heater designs, the radiation will be given as a function of a coordinate system in the plane of the target with the x-axis horizontal and the y-axis vertical. This means these axes are perpendicular to the sides of the target. In all cases only the relative amplitude of the radiation pattern will be considered where the maximum radiation is normalized to unity.

Since the target is square it is not unreasonable to assume that a square shaped heater would provide a more uniform radiation field on the target than a circular one. Figure 1 shows the relative intensity in the plane of the target for a solid circular and square heater disk. These curves were calculated by the use of our computer program. The calculated points are indicated by circles. The "H" on the x-axis marks the horizontal position of the side of the target. The "D" marks the distance from the center to a corner of the target. The curves for the square and round heaters differ at most by only a few percentage points. One would expect some asymmetry in the radiation pattern from a square heater. However, in Figure 2 the radiation along the horizontal axis (indicated by the open circles) and the radiation along the diagonal of the target (indicated by the open squares) are shown. We can not see any asymmetry at the level of detail given in Figure 2.

Real heaters are not solid disks but consist of some sort of spiral or concentric circular design. In Figure 3 the radiation pattern due to a solid square disk and 2, 3, and 4 square concentric rings heaters are shown. The ring heaters' widths were 12.7 mm, 6.35 mm, and 6.35 mm (0.5, 0.25, and 0.25 in.) and the separations were 6.35 mm, 6.35 mm, and 3.17 mm respectively. There is very little difference between these different configurations.

In Figure 4 the radiation pattern due to a solid square disk and two cones are shown. The cones consist of three concentric rings. The second ring is 1.27 cm closer to the target than the center disk. The third ring is 2.54 cm closer to the target than the center disk. For the curve marked with filled circles (indicated by "Cone") the center of the cone is 7.62 cm from the target. The curve labeled "Cone-2" is the same cone but it is 6.35 cm from the target.

In Figure 5 the impact of moving the solid square heater from a separation of 7.62 cm to 3.81 cm are shown. For the closer separation the relative radiation field that falls off much more rapidly.

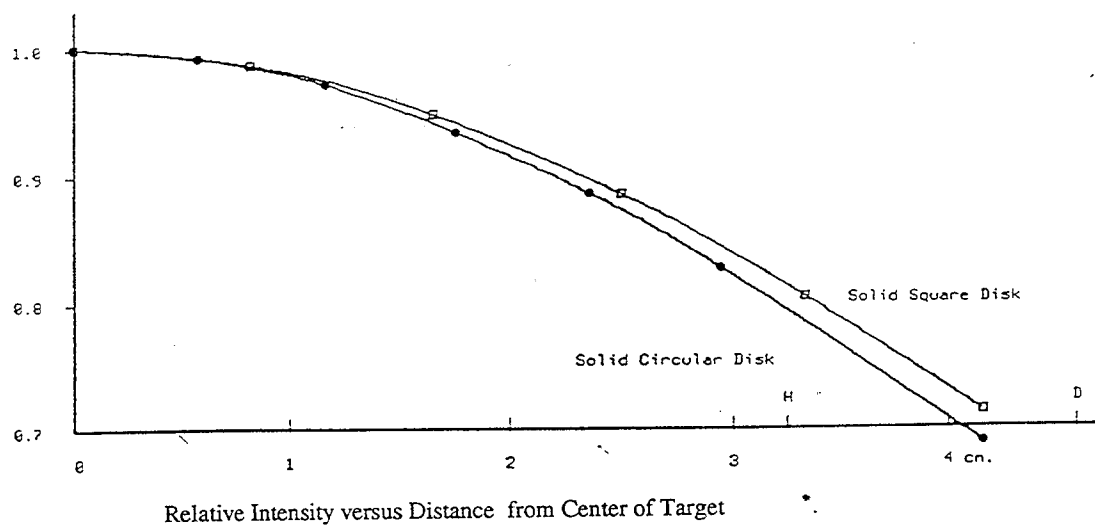


Figure 1. Solid Circular Disk and Solid Square Disk

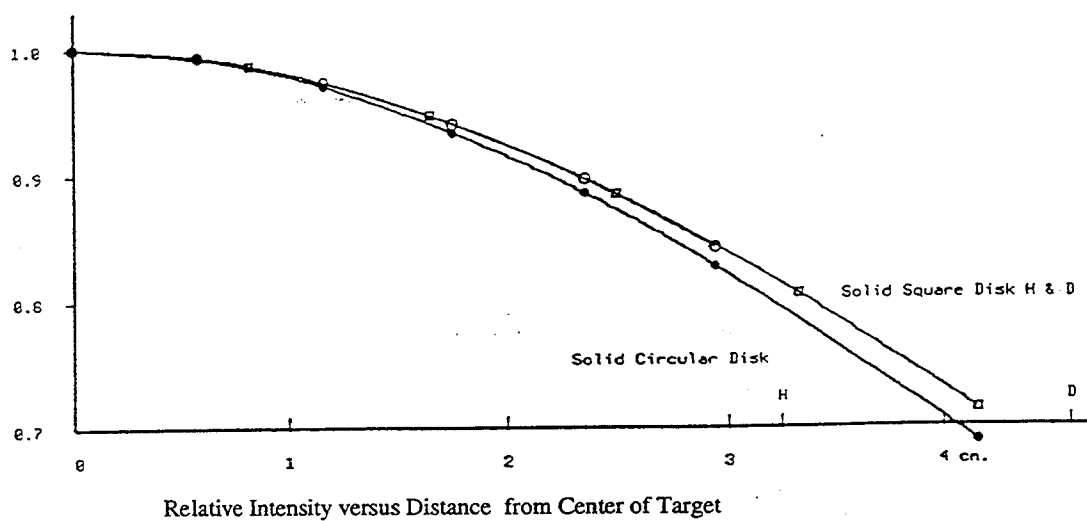


Figure 2. Solid Circular Disk and Solid Square Disk Horizontally and Diagonally

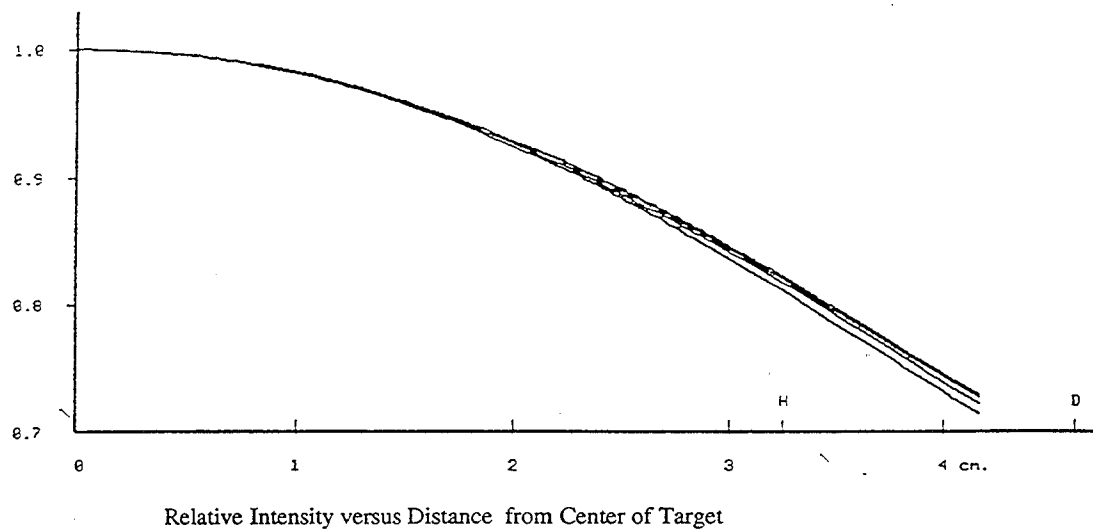


Figure 3. Solid Circular Disk and 2, 3, 4 Rings Source

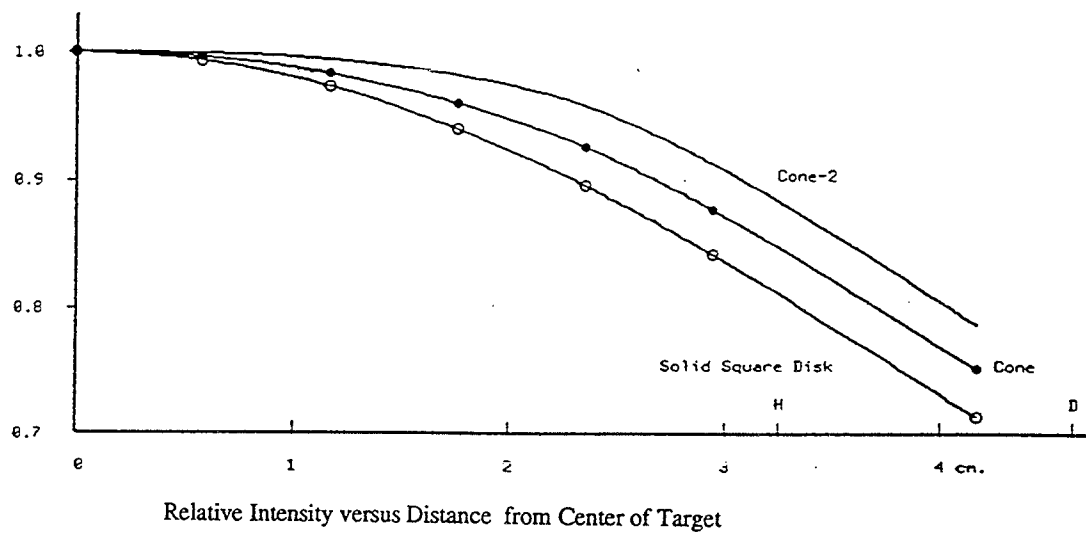


Figure 4. Cone, Cone 2, and Solid Square Disk

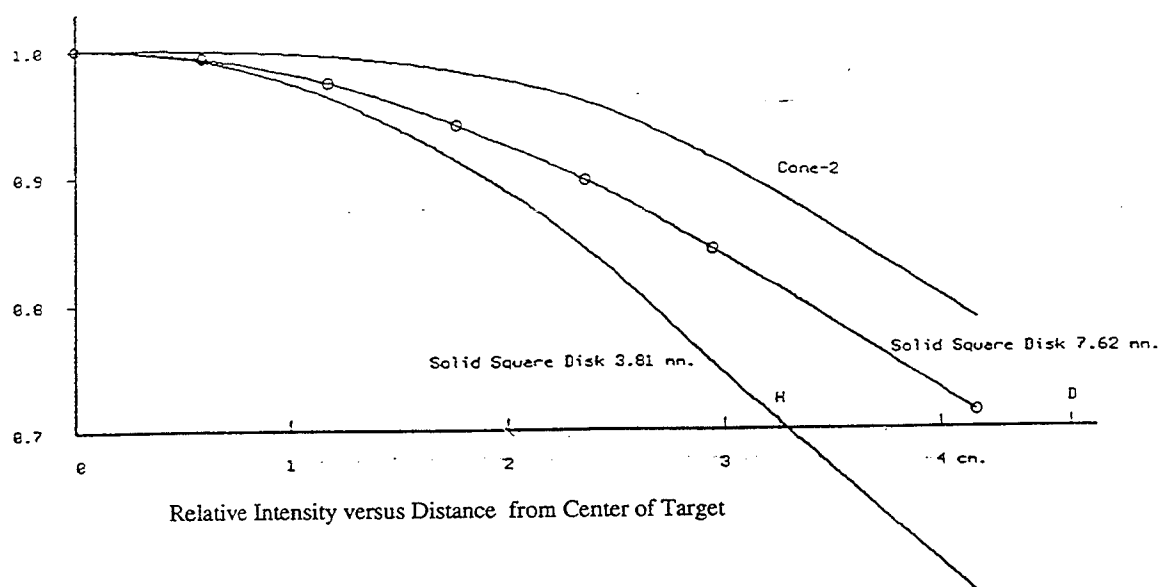


Figure 5. Square Square Disk 3.81 mm., Solid Square Disk 7.62 mm., and Cone 2

Based upon the above considerations, two heaters were ordered from commercial vendors, a tubular and a stainless steel heater. The one that had the radiation pattern closest to the ideal of a solid circular disk heater was the tubular heater shown in Appendix 3. The mounting of this heater in a smoke chamber furnace is shown in Figure 6.

III. Gauge

The ASTM E 662-83 standard calls for the use of an air cooled Gardon gauge with a 38.1 mm (1.5 in.) aperture. We propose to replace this air cooled gauge with a smaller (6.35 mm aperture) water cooled Gardon gauge. This type of gauge is used in the OSU calorimeter which is used by many organizations conducting FAA tests. This water cooled gauge should speed up the measurement process and improve the accuracy of the target radiation measurements.

We used the gauge provided by FAA to make all the measurements of the radiation profiles of the next section. FAA provided us with the manufacturer's calibration for this instrument (Appendix 1). It was "calibrated" (Appendix 2) at BFRL and found to have a slightly different calibration factor. The calibration factors differed by about 3%. Also, the effect of placing the gauge in the FAA mounting that resembles a target was determined to be negligible.

While a Gardon gauge will respond to radiation falling anywhere in its aperture, it does not measure the average field over its aperture except in special cases such as when a constant uniform field falls on its aperture. The most sensitive spot on a Gardon gauge is normally near the center of the gauge. Thus it is not surprising that the 38.1 mm aperture gauge indicated the same value for the radiation field as did the 6.35 mm gauge.

IV. Radiation profile

A. Radiation profile technique

The radiation profile technique used was similar to one used by the FAA in their round robin but it required closer spacing of the measurements. (Measurements were taken on approximately a 1.27 cm [0.5 in.] grid rather than a 2.54 cm [1 in.] grid.) The grid did not have exactly 1.27 cm spacing so as to avoid some possible systematic errors and to obtain a wider sampling of radial distance values.

B. Experimental results

Figure 7 shows the experimental results of horizontal scans of the relative radiation intensity for the tubular heater, the stainless steel heater, and the current smoke chamber heater compared to the ideal curve. From these curves it would appear that the tubular heater comes the closest to

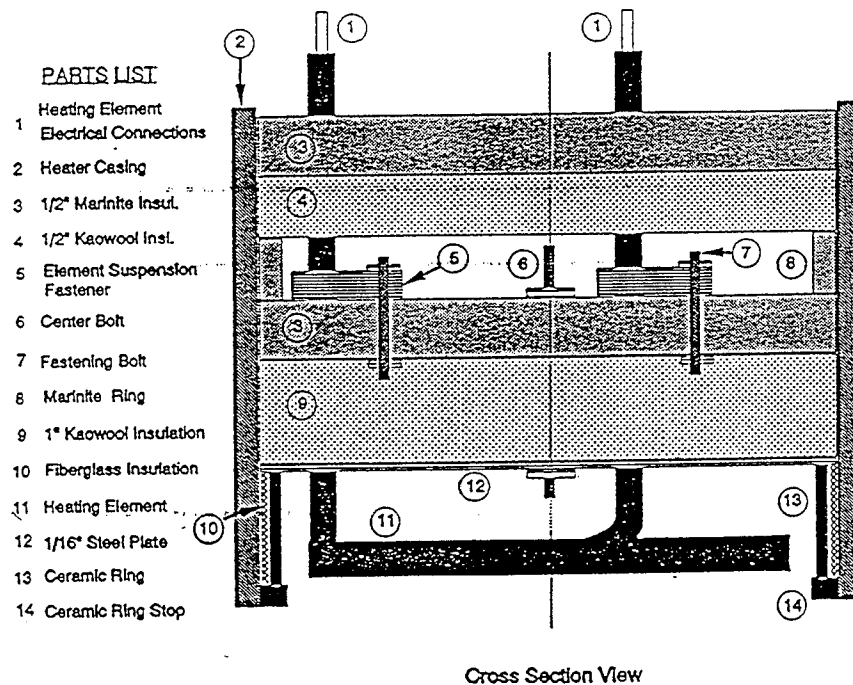


Figure 6. Modified NIST Smoke Chamber Heater Assembly

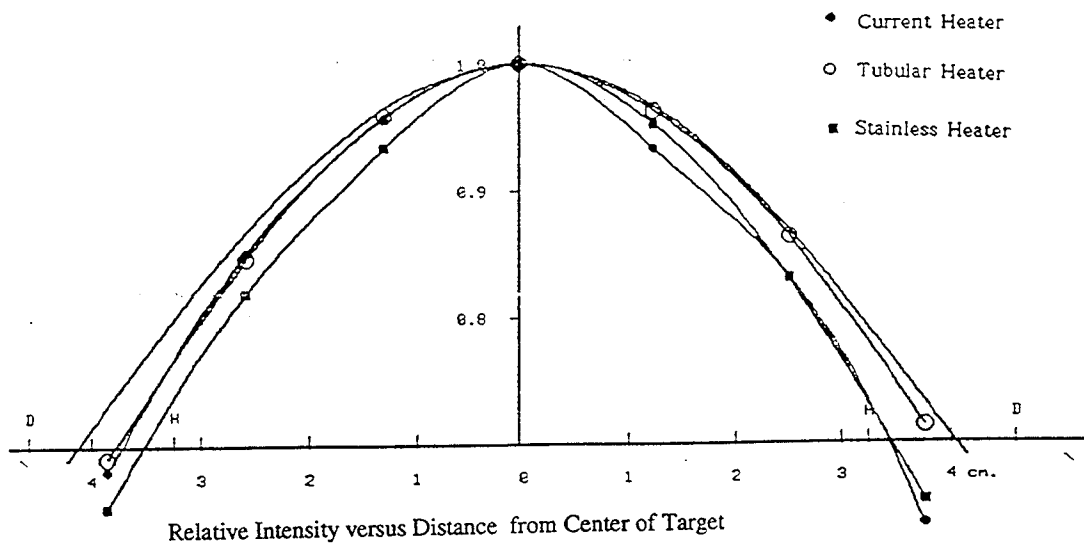


Figure 7. Horizontal Scan of Tubular, Stainless, and Current Heater Fields Compared to Ideal

the ideal.

Figure 8 shows the experimental results of vertical scans for the tubular heater, the stainless steel heater, and the current smoke chamber heater compared to the ideal curve. From these curves also it would appear that the tubular heater comes the closest to the ideal.

Figures 9 through 12 show the experimental results of radial scans compared to the ideal curve. Figure 9 shows the results for the tubular heater. Unlike the previous figures no curve is drawn through these data points. Figure 10 shows the results for the stainless steel heater. Figure 11 shows the results for the current smoke chamber heater. Figure 12 shows the results for the three heaters and the ideal. From these curves it would appear that the tubular heater comes the closest to the ideal.

Figures 13 through 15 shows the experimental results of radial scans (with position and power uncertainty indicated) compared to the ideal curve. The accuracy of the position measurements were ± 1.6 mm [1/16"]. This was considered reasonable when one considers that the size of the active area of the detector was 6.25 mm [1/4"]. From the "calibration report" we see that the smallest inaccuracy we can take for the power measurements is $\pm 5\%$. Figure 13 shows the results for the tubular heater. Figure 14 shows the results for the stainless steel heater. Figure 15 shows the results for the current smoke chamber heater. From these curves it would appear that the tubular heater comes the closest to the ideal.

We note that in the various ways of viewing the experimental data the tubular heater always appeared to come closer to the ideal solid circular disk heater than any of the others. When the measurement uncertainties are included, the picture becomes less clear but the tubular heater still appears to be nearer the ideal.

C. Estimation of average power

The ideal radiation curve for a solid cylindrical disk can be approximated by a polynomial. If a fourth order polynomial is used, the field at radial distance r from the axis of symmetry can be written as

$$F(r) = F_0 [1 + ap + bp^2 + cp^3 + dp^4] \quad (1)$$

where p is r/w , $2w$ is width of the target, and F_0 is the radiation field where r is zero.

The requirement of cylindrical symmetry implies that the slope of the field be zero when r is zero. Therefore, it follows that "a" is zero. For computational convenience, we set "c" equal to zero since the integrals associated with this term are difficult. Therefore, the above equation becomes

$$F(r) = F_0 [1 + bp^2 + dp^4] \quad (2)$$

We wish to compute the average radiation field over the area of the target. The average field is

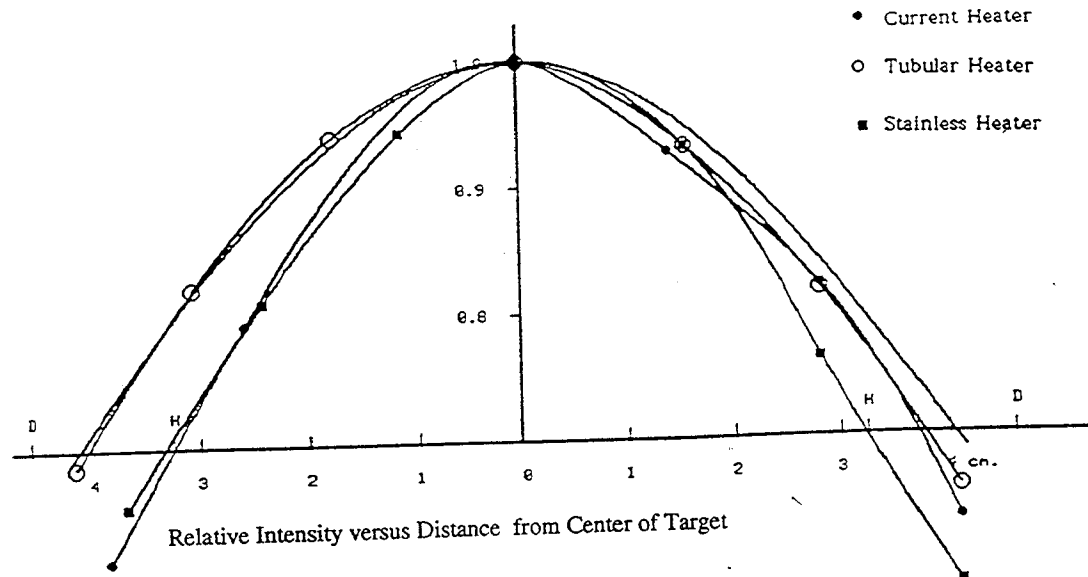


Figure 8. Vertical Scan of Tubular, Stainless, and Current Heater Fields Compared to Ideal

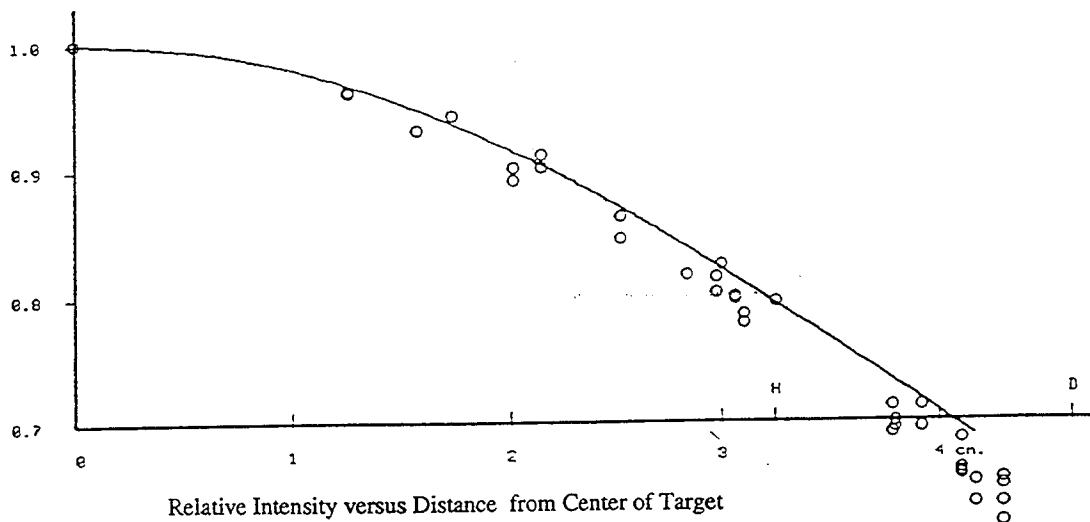
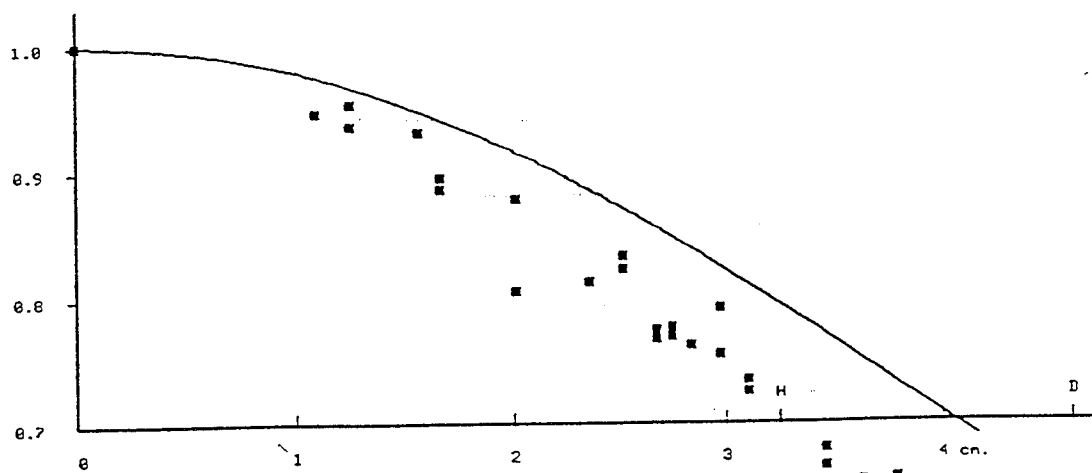
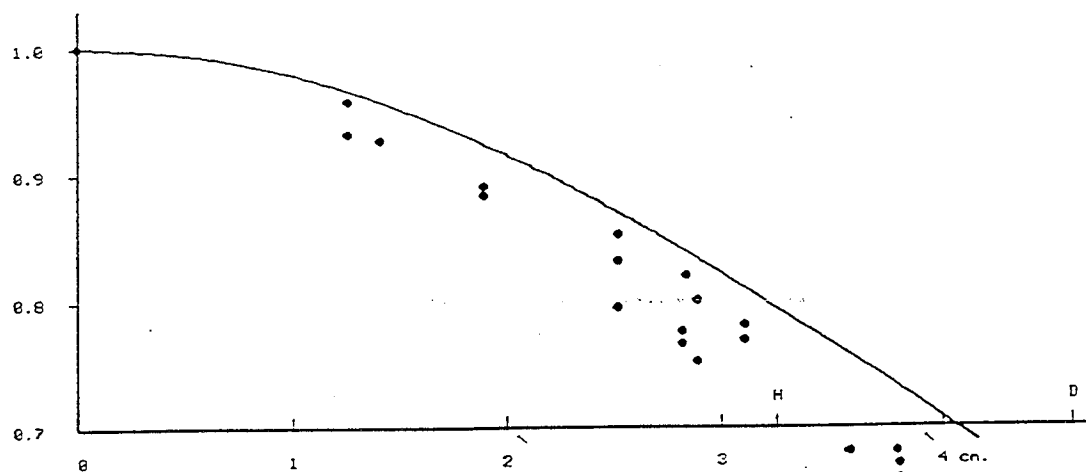


Figure 9. Radial Scan of Tubular Heater Fields Compared to Ideal



Relative Intensity versus Distance from Center of Target

Figure 10. Radial Scan of Stainless Heater Fields Compared to Ideal



Relative Intensity versus Distance from Center of Target

Figure 11. Radial Scan of Current Heater Fields Compared to Ideal

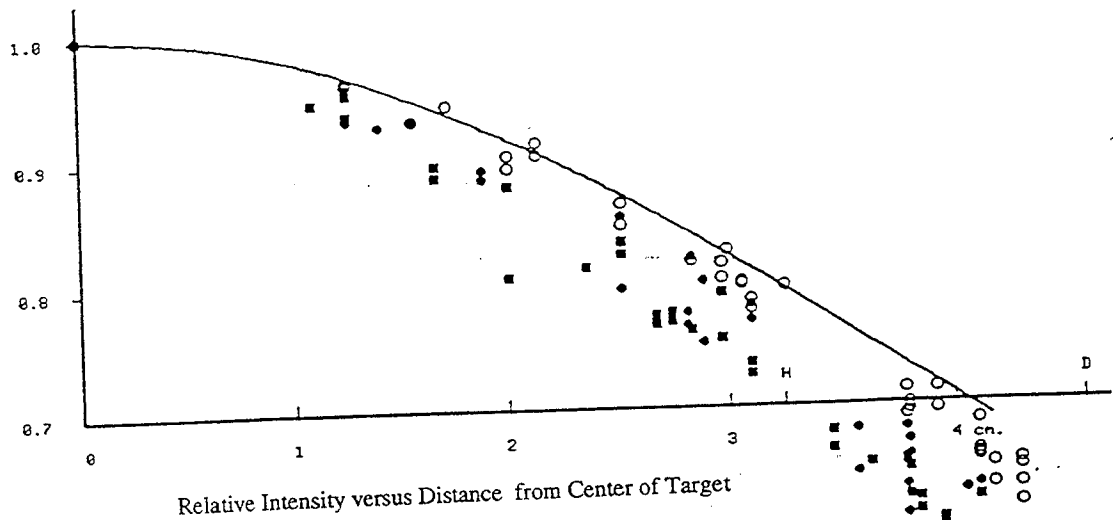


Figure 12. Radial Scan of Tubular, Stainless, and Current Heater Fields Compared to Ideal

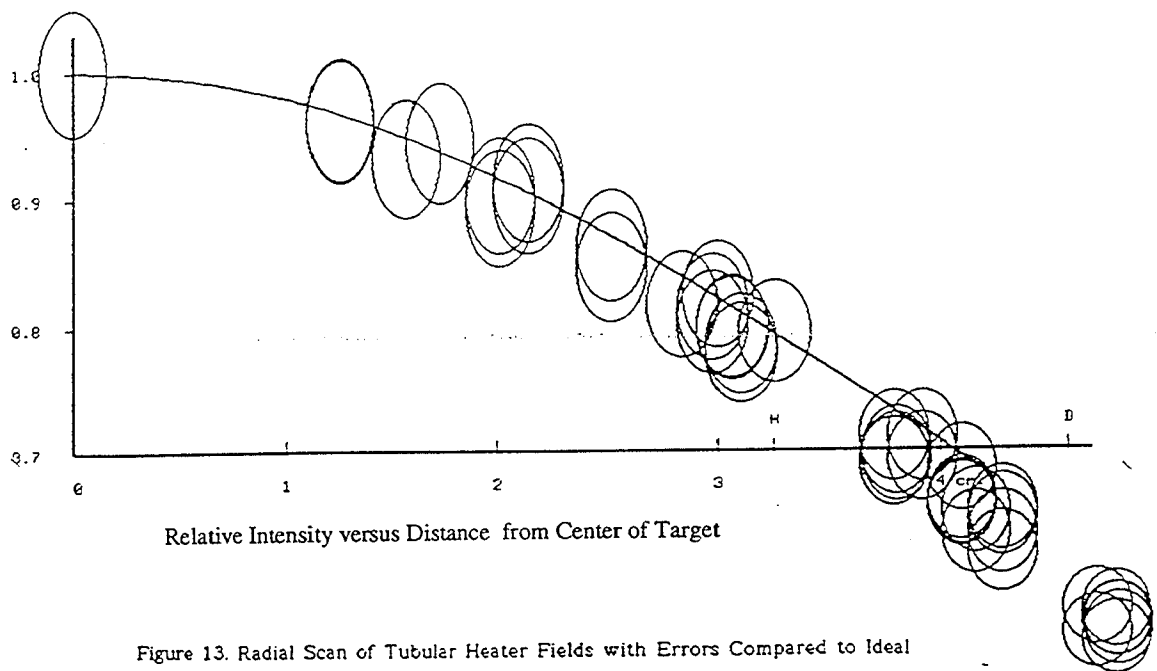


Figure 13. Radial Scan of Tubular Heater Fields with Errors Compared to Ideal

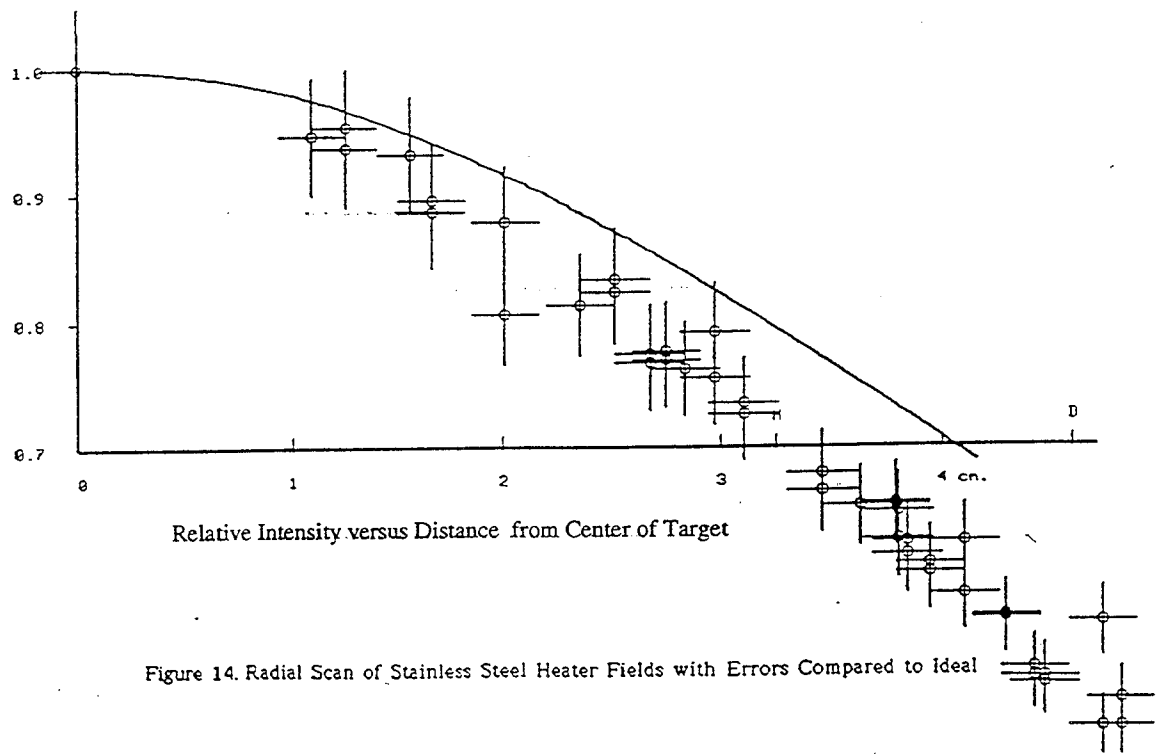


Figure 14. Radial Scan of Stainless Steel Heater Fields with Errors Compared to Ideal

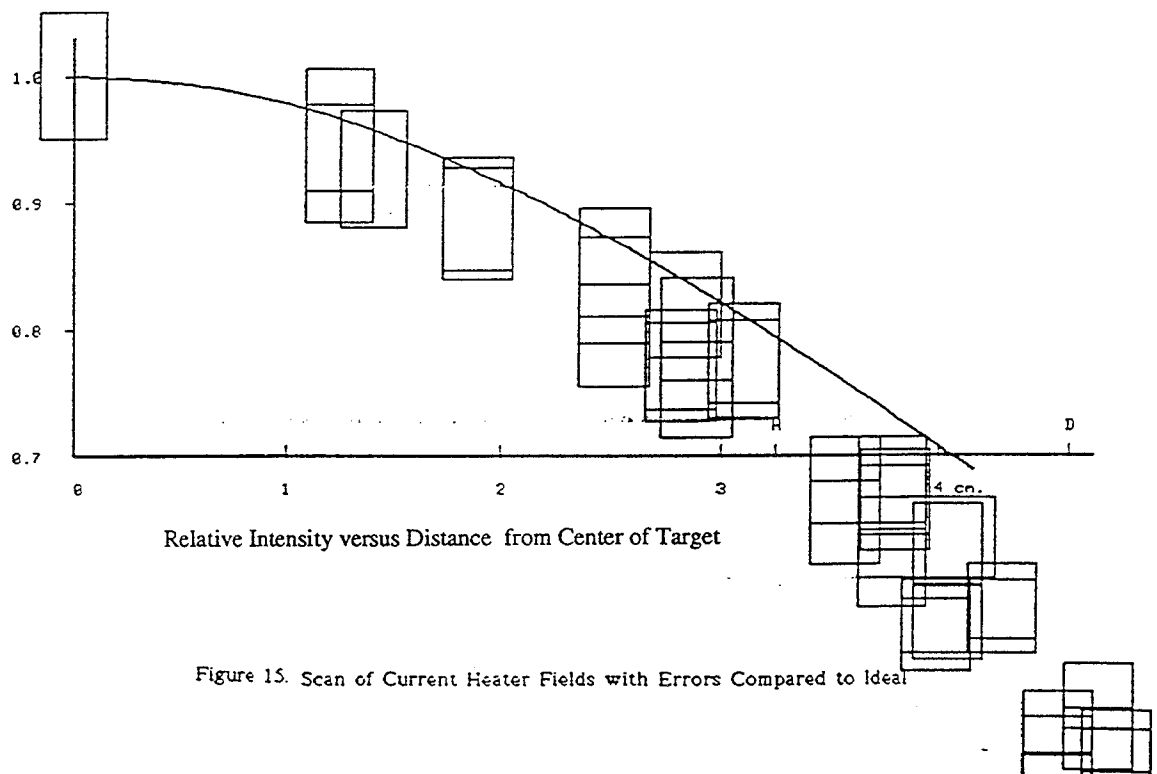


Figure 15. Scan of Current Heater Fields with Errors Compared to Ideal

given by the equation

$$\bar{F} = \frac{1}{\text{area}} \int F(r) dA \quad (3)$$

where the area of integration is the area of the target. This can be written as

$$\bar{F} = \bar{F}_r + \bar{F}_c \quad (4)$$

The first term is the value of the integral over the area of a circle of radius w in the target. It can be written as

$$\bar{F}_r = \frac{1}{4w^2} \int_0^{2\pi} \int_0^w F(r) r dr d\theta \quad (5)$$

The second term of equation 4 is the integration over the area in the target square outside the circle. This term is equal to four times the integral of one corner. Thus

$$\bar{F}_c = \frac{1}{w^2} \int_0^w \int_{x_1}^w F(r) dx dy \quad (6)$$

where

$$x_1 = \sqrt{w^2 - y^2} \quad (7)$$

We find after doing these integrals that

$$F = F_0 \left[1 + \frac{2}{3} b + \left(\frac{\pi}{12} + \frac{28}{45} - \frac{3\pi}{32} \right) d \right] \quad (8)$$

If the values of

$$b = -0.191$$

and

$$d = 0.018$$

are used and compare the theoretical radiation values to the polynomial the results given in Table 1. are obtained.

r(in units of w)	0	.2	.4	.6	.8	1.0	1.414
radiation	1.0	.992	.970	.933	.885	.827	.689
polynomial	1.0	.992	.970	.934	.885	.827	.690

Table 1. Comparison of Polynomial Curve Fit to Radiation Calculation.

This polynomial seems to be a reasonably good fit to our theoretical ideal curve.

Therefore, if the above values for b and d are substituted into equation 8 and evaluated it follows that

$$F = .883 F_0 \quad (9)$$

In other words, the average value for the ideal radiation field is equal to approximately 0.88 times the peak or central value. While in principle, one could determine b and d for the tubular heater, the accuracy of the measurements do not justify this additional effort and one has a reasonable approximation using Eq. (9).

D. Effect of pilot burner's structure

In response to a question as to how much incident radiation is blocked by the pilot burner structure we provide the following. When the pilot burner is off, its only effect is to block a small fraction of the incident radiation from striking the target. The maximum total area blocked is 1.8 sq. cm. The total area of the target is 41.94 sq. cm. Thus the fraction of the target blocked by the burner is .043 (4.3%). The importance of this is further reduced due to the fact that the area blocked is near the edge of the target where the radiation is the weakest.

V. Smoke chamber measurements

Per FAA's request, we measured four FAA samples before and after changes to the smoke chamber. We list the results below without comment on the significance of the changes owing to the lack of a detailed error analysis of the smoke chamber and its method. Such an error analysis is beyond the scope of the current project.

Case 1. Measurements of FAA samples before any changes in the smoke chamber. These results are given in table 2.

	Maximum specific optical density, D_m				
	test 1	test 2	test 3	average	std. dev.
Epoxy fiberglass	160	146	146	151	8.1
Phenolic fiberglass	11	11	11	11	0
Test Panel "C" - 915	188	196	196	193	4.6
Test Panel/200	167	160	167	165	4

Table 2. Measurements of FAA Samples Using Unmodified Smoke Box.

Case 2. Measurements of FAA samples after the changes to the heater and the detector with the measured field set to equal 2.5 w/sq. cm. These results are given in table 3.

	Maximum specific optical density, D_m				
	test 1	test 2	test 3	average	std. dev.
Epoxy fiberglass	146	167	167	160	12.1
Phenolic fiberglass	4	7	4	5	1.7
Test Panel "C" - 915	171	181	185	179	7.2
Test Panel/200	167	167	174	169	4.0

Table 3. Measurements of FAA Samples Using Modified Smoke Box.

VI. Summary

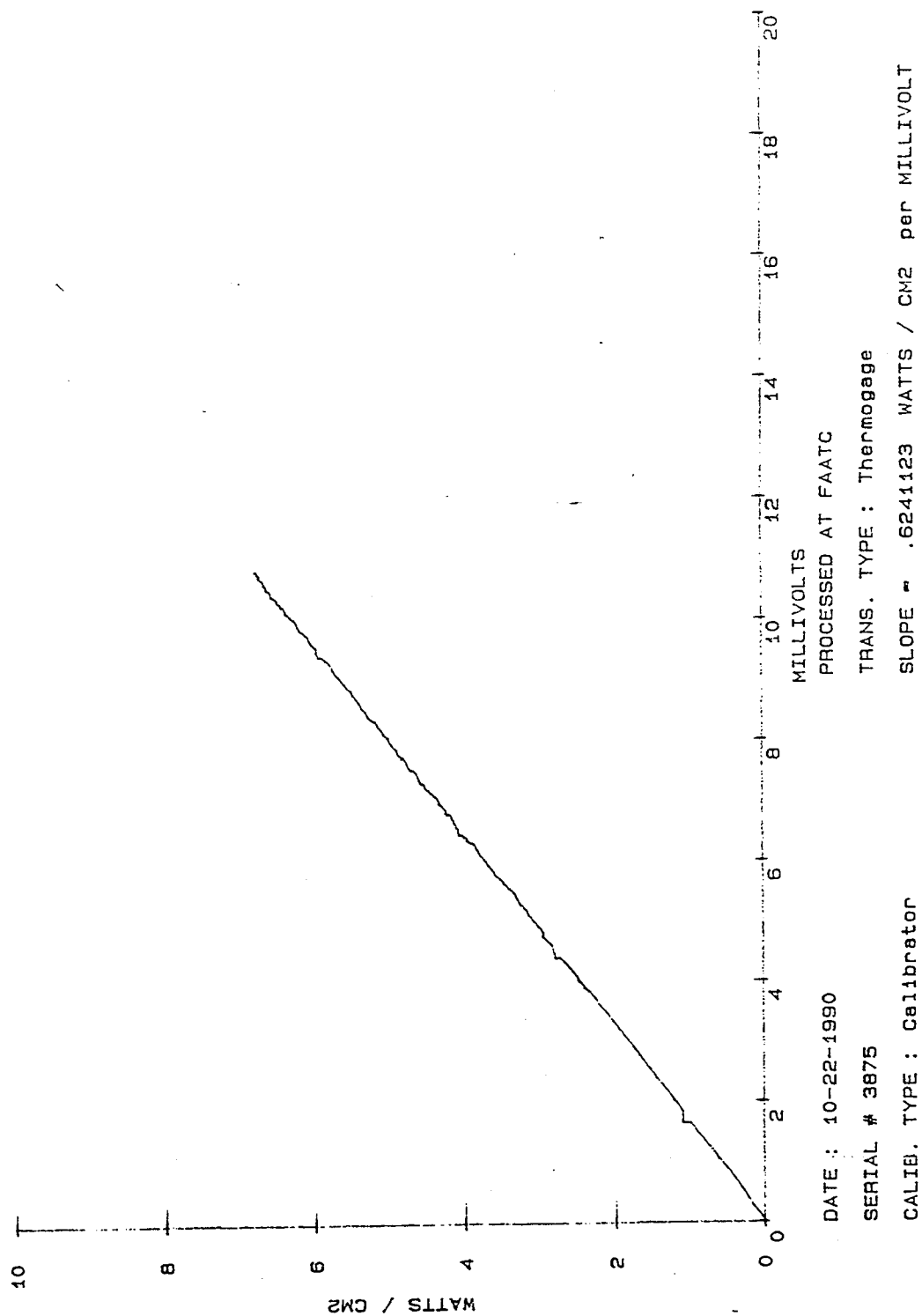
We have provided the following:

- 1) a demonstration of a prototype of a heater that will probably provide a more uniform radiation field on the target specimen,
- 2) a demonstration of the use of a gauge similar to the one used in the OSU calorimeter for use in the smoke box for measuring the heat flux,
- 3) a method for using this heater and gauge that allows one to use the measurement of the radiation field at the center of the specimen to infer the average radiation field over the specimen, and
- 4) finally, in Appendix 4, suggested changes to the FAA's "Smoke Test for Cabin Materials."

Reference

[1] ASTM E 662-83 Standard Test Method for Specific Optical Density of Smoke Density of Smoke Generated by Solid Materials, **1990 Annual Book of ASTM Standards**, volume 4.07, p563

Appendix 1: Manufacturer's Calibration Curve of FAA's Gauge



11/8/91

Richard Smith
NIST
c/o FAA Smoke Chamber Heat Flux Gauge

Dear Mr. Smith,

Per your request I have calibrated your 1" Gardon type heat flux gauge, Medtherm 64-2-20 with serial number 3875. A substitution technique was used to calibrate the gauge in an infrared radiant field at flux levels to nominally 4 W/cm^2 . A schematic of the test arrangement is shown in Fig. 1.

The radiant field is produced by a downward-facing conical electric heater. The flux level at the measurement point is established with our standard transfer gauge --- a Gardon gauge which is periodically calibrated against our standard self-calibrating reference radiometer. This reference radiometer has been well characterized with respect to accuracy by the Radiometric Physics Division, National Institute of Standards and Technology. Its accuracy is within 3 percent over the range 1 mW/cm^2 to 0.9 W/cm^2 . Cooling water at 25 ± 0.2 degrees C was supplied to each sensor. The flow rate through the Gardon gauges was maintained at approximately 17 ml/s. Water at 25 ± 1 degrees C was supplied to the copper plate that surrounds the heater. The lower face of this plate is painted black.

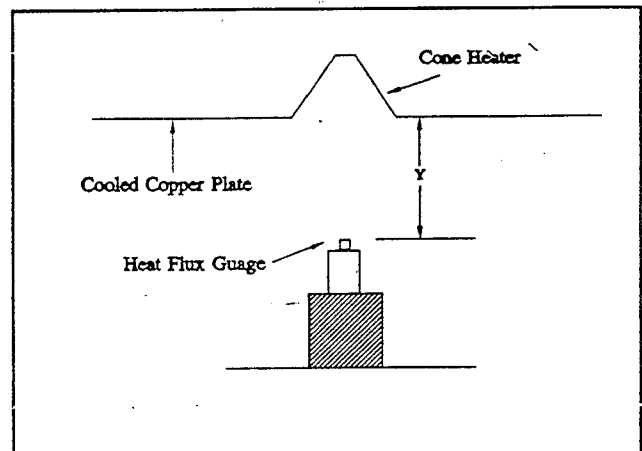


Figure 1 Schematic of test arrangement.

Based on assumptions of linearity of the transfer gauge and system uncertainties, we expect overall accuracy of within 5 percent for the calibration range. Future analysis is expected to address this more thoroughly.

The calibration results are presented in tabular form. Note that the flux level was varied in two ways; 1) the temperature of the heater was fixed while the distance between the heater and gauge was varied, and 2) the separation distance was fixed and the temperature of the heater was varied. The response curve, is included after the data table.

The results of this test program should not be considered as an official National Institute of Standards and Technology calibration. If you have any questions regarding this calibration, please contact me at (301) 975-6667.

Sincerely,


Darren L. Lowe
Building and Fire Research Laboratory

REPORT OF TEST --- HEAT FLUX GAUGE CALIBRATION

Date of Test: 11/8/91

Owner: FAA

Model:

Serial Number: 3875

Comments:

Y (mm)	Flux (W/cm ²)	Output (mV)	T _{heater} (°C)
294	-0.002	-0.003	off
294	0.80	1.310	850
294	1.13	1.852	850
244	1.34	2.183	850
222	1.68	2.757	850
194	2.23	3.649	850
163	3.13	5.099	850
130	3.38	5.491	850
123	2.18	3.574	717
123	1.66	2.683	643
123	0.82	1.324	477

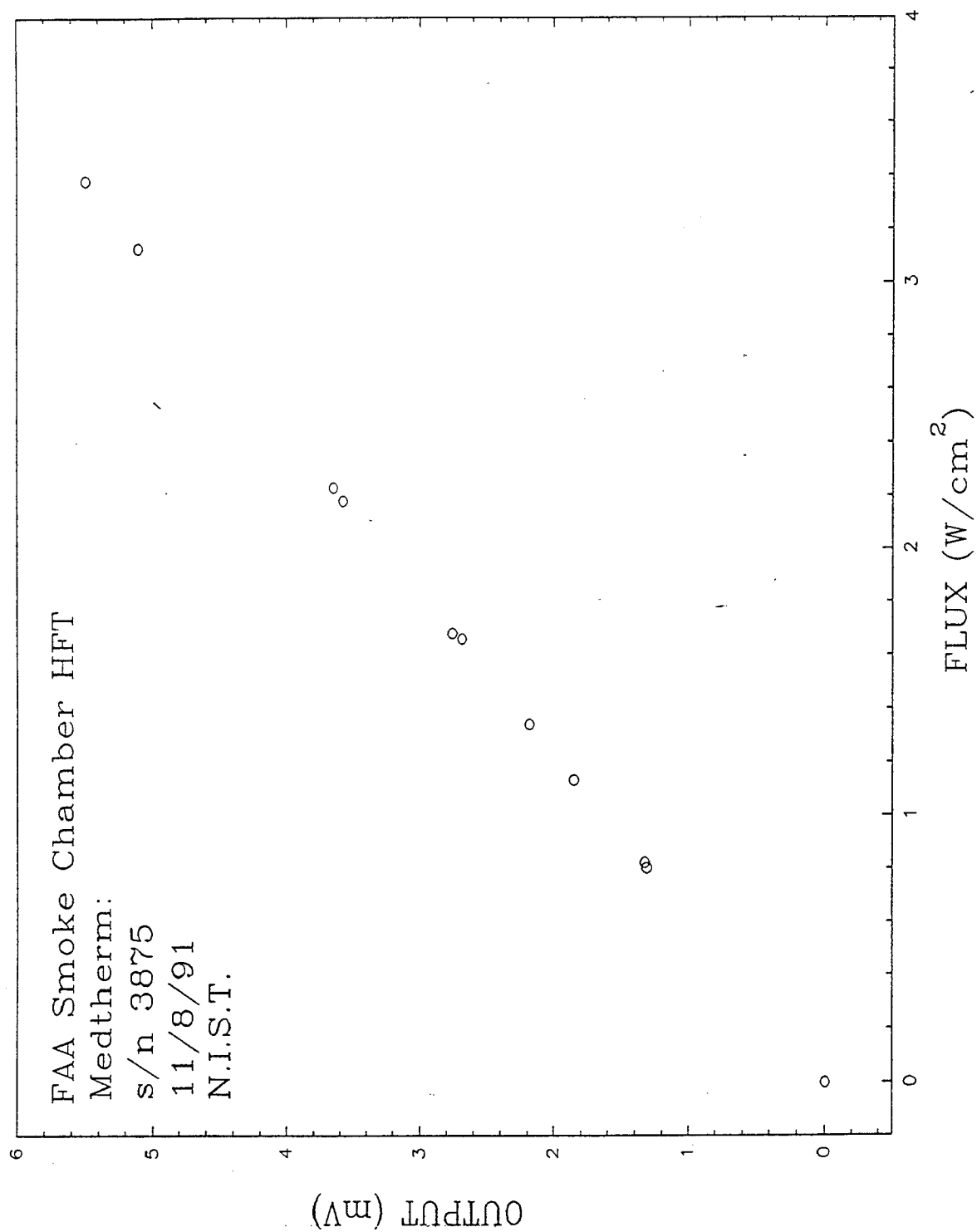


Figure 2 Response curve for heat flux gauge.

ADD OTHERWISE SPECIFIED
USE THE FOLLOWING

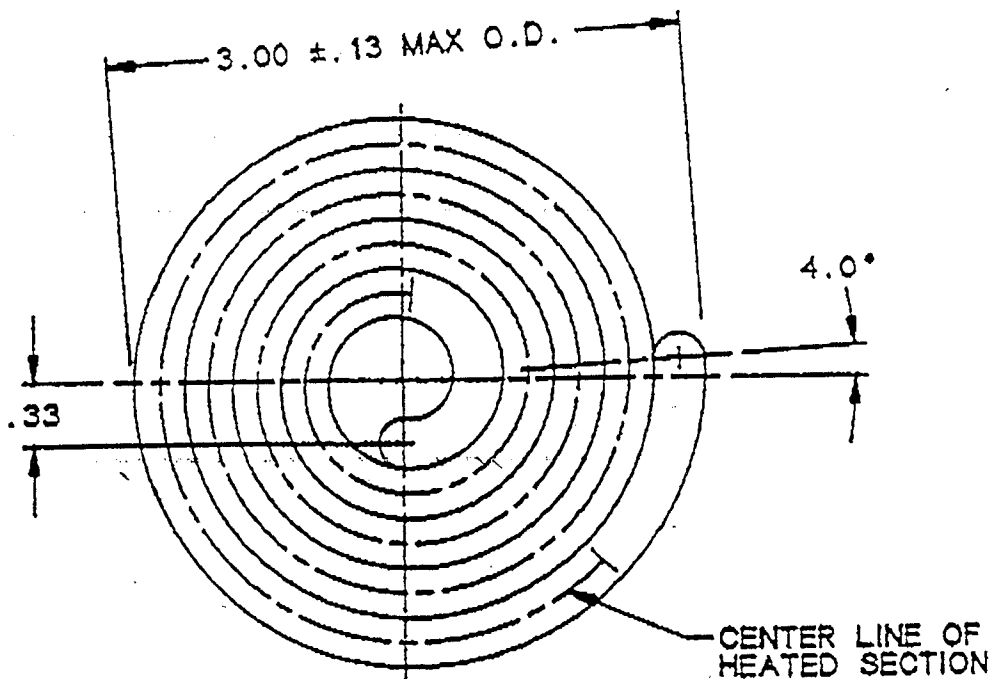
TOLERANCES		
FRACTIONS	DECIMALS	ANGLES
	.XX	
	.XXX ±	±

TITLE

FORMED TUBULAR HEATER

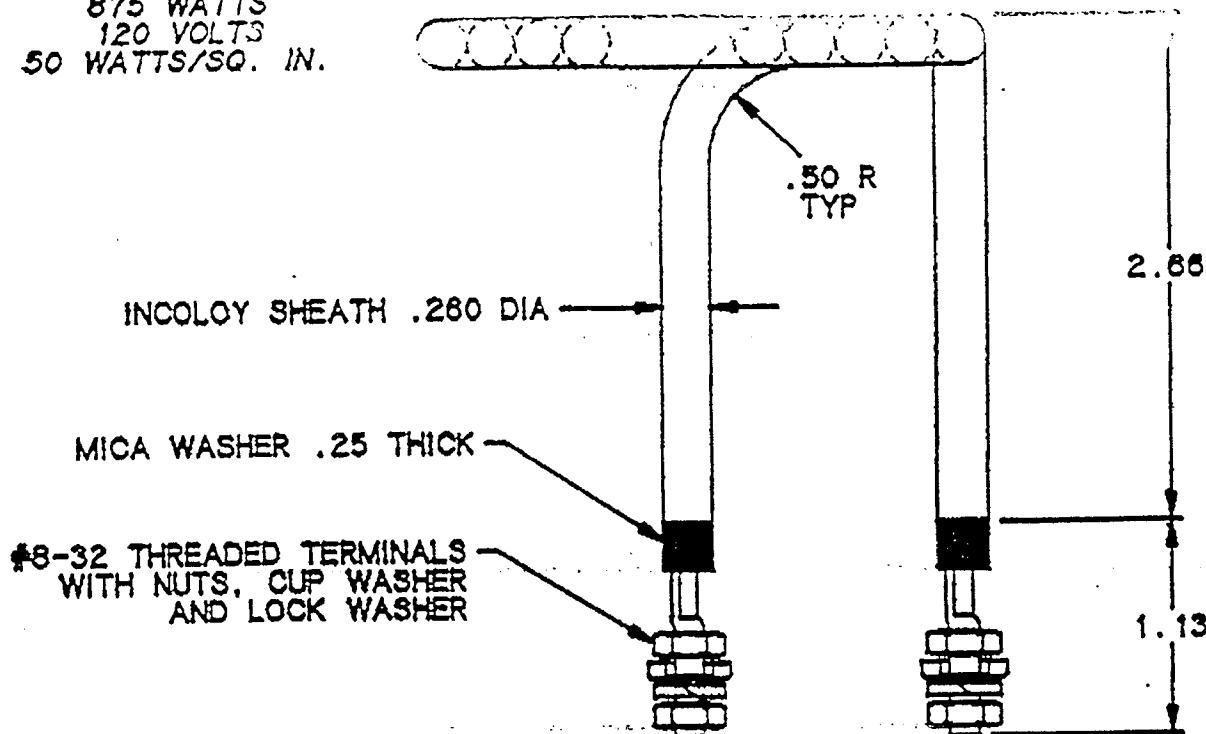
FIRST MADE FOR U.S. DEPT. OF COMMERCE

40A132880
CONT ON SHEET F SH NO



1

875 WATTS
120 VOLTS
50 WATTS/SQ. IN.



REVISIONS	APPROVALS	WELLMAN Thermal Systems Corporation SHELBYVILLE, INDIANA
	<i>R. L. Boyce</i>	
	MADE BY: D. BOYCE 8-20-91	
	ISSUED: 8-21-91	
PRINTS TO	40A132880	CONT ON SHEET F SH NO.

FORMING, 40-22 334079

Appendix 4: Suggested New Wording for FAA's "Smoke Test for Cabin Materials"

The following changes are suggested if the new heater and gauge are required for the FAA smoke test.

Delete footnote 6 "Furnace model . . . acceptable."

Delete footnote 7 "Heating element . . . acceptable."

Delete footnote 9 "The construction . . . ASTM F814-83."

Delete footnote 11 "A thermocouple system . . . density gauge."

Change

"6.3.1.6.2 Heating Element -- The heating element shall consist of a coiled **wire** capable of dissipating about 525 W. . . ."

to

"6.3.1.6.2 Heating Element -- The heating element shall consist of a coiled **rod** capable of dissipating about 525 W **or more**. . . ."

Change

"6.3.1.6.4 Heat Flux Density Gauge -- An **air**-cooled heat flux density gauge shall be provided for calibrating the output of the radiant heat furnace. The heat flux density gauge shall be a circular foil type, the operation of which was described by gardon¹⁰

Compressed air . . . contact. The circular receiving surface of the heat flux... FAA Administrator."

to

"6.3.1.6.4 Heat Flux Density Gauge -- A **water**-cooled heat flux density gauge shall be provided for calibrating the output of the radiant heat furnace. The heat flux density gauge shall be a circular foil type, the operation of which was described by gardon¹⁰

The circular receiving surface of the heat flux... FAA Administrator."

Delete the following

"6.6.2.2 . . . With the chamber . . . (93±3°C)."

NIST-114A (REV. 3-90)		U.S. DEPARTMENT OF COMMERCE NATIONAL INSTITUTE OF STANDARDS AND TECHNOLOGY		1. PUBLICATION OR REPORT NUMBER NISTIR 4917
BIBLIOGRAPHIC DATA SHEET		2. PERFORMING ORGANIZATION REPORT NUMBER		
		3. PUBLICATION DATE September 1992		
4. TITLE AND SUBTITLE New Heater and Flux Gauge for the NBS Smoke Box				
5. AUTHOR(S) Richard L. Smith				
6. PERFORMING ORGANIZATION (IF JOINT OR OTHER THAN NIST, SEE INSTRUCTIONS) U.S. DEPARTMENT OF COMMERCE NATIONAL INSTITUTE OF STANDARDS AND TECHNOLOGY GAITHERSBURG, MD 20899			7. CONTRACT/GRANT NUMBER	
			8. TYPE OF REPORT AND PERIOD COVERED	
9. SPONSORING ORGANIZATION NAME AND COMPLETE ADDRESS (STREET, CITY, STATE, ZIP) Federal Aviation Administration FAA Technical Center Atlantic City Airport, NJ 08405				
10. SUPPLEMENTARY NOTES				
11. ABSTRACT (A 200-WORD OR LESS FACTUAL SUMMARY OF MOST SIGNIFICANT INFORMATION. IF DOCUMENT INCLUDES A SIGNIFICANT BIBLIOGRAPHY OR LITERATURE SURVEY, MENTION IT HERE.) Improvements of the heater and the heat flux detector used in the FAA's Smoke Chamber test protocol are described. Heater designs were evaluated and two heaters were obtained and evaluated. This report covers various aspects of analysis and gives details on the heater that may provide a more uniform radiation field on the target specimen. The use of a smaller gauge, similar to the one used in the OSU calorimeter, in the smoke box for measuring the heat flux is discussed. Finally, a method that allows one to use the measurement of the radiation field at the center of the target specimen to infer the average radiation field over the specimen is presented.				
12. KEY WORDS (6 TO 12 ENTRIES; ALPHABETICAL ORDER; CAPITALIZE ONLY PROPER NAMES; AND SEPARATE KEY WORDS BY SEMICOLONS) Smoke chamber test, smoke measurement				
13. AVAILABILITY <input checked="" type="checkbox"/> UNLIMITED <input type="checkbox"/> FOR OFFICIAL DISTRIBUTION. DO NOT RELEASE TO NATIONAL TECHNICAL INFORMATION SERVICE (NTIS). <input type="checkbox"/> ORDER FROM SUPERINTENDENT OF DOCUMENTS, U.S. GOVERNMENT PRINTING OFFICE, WASHINGTON, DC 20402. <input checked="" type="checkbox"/> ORDER FROM NATIONAL TECHNICAL INFORMATION SERVICE (NTIS), SPRINGFIELD, VA 22161.			14. NUMBER OF PRINTED PAGES 30	
			15. PRICE A03	

ELECTRONIC FORM